Cancer Letters 466 (2019) 39–48

Contents lists available at ScienceDirect

Cancer Letters

journal homepage: www.elsevier.com/locate/canlet

Original Articles

NRF2 SUMOylation promotes *de novo* serine synthesis and maintains HCC tumorigenesis

Haoyan Guo[a,b,c,1], Jiaqian Xu[a,1], Quan Zheng[a], Jianli He[a], Wei Zhou[a], Kezhou Wang[a], Xian Huang[a], Qiuju Fan[a], Jiao Ma[a], Jinke Cheng[a], Wenhan Mei[a,**], Rong Xing[b,***], Rong Cai[a,*]

[a] Department of Biochemistry & Molecular Cell Biology, Shanghai Jiao Tong University School of Medicine, Shanghai, 200025, China
[b] Department of Pathophysiology, Dalian Medical University, Dalian, 116085, China
[c] Department of Pathology, Beijing Obstetrics and Gynecology Hospital, Capital Medical University, Beijing, 100026, China

ARTICLE INFO

Keywords:
Nuclear factor erythroid-2 related factor 2
Small ubiquitin-like protein
Serine synthesis
Hepatocellular carcinoma
Reactive oxygen species

ABSTRACT

Nuclear factor erythroid-2 related factor 2 (NRF2) is a pivotal transcription factor that maintains cellular redox homeostasis and facilitates the development of malignant tumor phenotypes. At the molecular level, NRF2 promotes *de novo* serine synthesis and SUMOylation affects its function. Our results indicated that the SUMO1 acceptor site of NRF2 is the conserved lysine residue 110 (K110), and that NRF2 SUMOylation deficiency inhibited tumorigenesis in hepatocellular carcinoma (HCC). Mechanistically, NRF2 SUMOylation promoted *de novo* serine synthesis in HCC by enhancing the clearance of intracellular reactive oxygen species (ROS) and upregulating phosphoglycerate dehydrogenase (PHGDH). More importantly, serine starvation increased the level of NRF2 SUMOylation, leading to sustained HCC growth. Collectively, our results indicate the presence of a novel NRF2 SUMOylation-mediated signaling process that maintains HCC tumorigenesis in normal conditions and in response to metabolic stress.

1. Introduction

Nuclear factor erythroid-2 related factor 2 (NRF2, also known as NFE2L2) is a transcription factor that facilitates the development of malignant phenotypes in multiple types of cancers [1]. Cancer cells exhibit at least two distinctive metabolic traits — an enhanced tolerance to oxidative stress and an increased rate of biosynthesis to support increased cell proliferation [1]. The NRF2 pathway is important in healthy cells because it maintains intracellular redox homeostasis [2]. Recent studies have reported that NRF2 also has a key role in regulating cancer cell metabolism [2,3]. In particular, abnormal activation of the NRF2 pathway in cancer cells leads to reprogramming of intermediary metabolism so that it supports cancer cell proliferation and tumorigenesis [3–6].

Constitutive *NRF2* activation occurs in 14% of human cells with hepatocellular carcinoma (HCC) [7,8]. Studies of a rat model of human HCC indicated that autophagy deficiency and then p62 accumulation caused continual activation of the NRF2 pathway [9], and this contributed to the onset and progression of preneoplastic lesions towards malignancy [10]. Another study of the rat resistance hepatocyte model demonstrated that the onset of *Nrf2* mutations is an early event in pathogenesis that promotes HCC progression and development [11]. A recent study using *Nrf2* knockout mice demonstrated that NRF2 is a crucial driver for diethylnitrosamine-induced hepatocellular carcinogenesis [12], and that mutations in *NRF2* are related to short survival times in HCC patients [12].

The serine synthesis pathway (SSP) is dysregulated in many cancers [13], and NRF2 has a pivotal role in regulation of serine synthesis in a substantial fraction of human non-small cell lung cancer cells (NSCLCs) [6]. Cancer cells often require *de novo* synthesis of serine from glucose, even in the presence of extracellular serine [13–15]. Serine fuels cellular glycine synthesis and nucleotide metabolism, and facilitates the folate cycle and amino acid transport in cancer cells [13]. Serine starvation reduces the activity of pyruvate kinase 2 (PKM2) and increases the amount of glucose-derived carbon fluxes into serine synthesis to support cancer cell proliferation [16]. Activation of p53-p21 induces metabolic remodeling and supports the proliferation of cancer cells during serine starvation [17]. Phosphoglycerate dehydrogenase

* Corresponding author.
** Corresponding author.
*** Corresponding author.
E-mail addresses: jymeiwh@shsmu.edu.cn (W. Mei), xr_blsl@dlmedu.edu.cn (R. Xing), rongcai@shsmu.edu.cn (R. Cai).
[1] These authors contribute equally to this manuscript.

https://doi.org/10.1016/j.canlet.2019.09.010
Received 13 June 2019; Received in revised form 20 August 2019; Accepted 18 September 2019

(PHGDH) is the rate-limiting enzyme for the *de novo* synthesis of serine, and p53-mediated repression of PHGDH is crucial for blocking the apoptosis of cancer cells upon serine starvation [18]. Although NRF2 is a crucial regulator of serine synthesis, the effect of altering NRF2 activity in response to serine starvation is still unknown.

In healthy cells, NRF2 binds with adaptor protein Kelch-like ECH-associated protein 1 (KEAP1) in the cytoplasm, which then recruits E3 ubiquitin ligase Cullin 3 (CUL3), thus facilitating the rapid degradation of NRF2 by proteasomes [19,20]. Upon stress, NRF2 separates from KEAP1 and translocates into the nucleus, where it induces the expression of target genes [21]. In addition, other E3 ubiquitin ligase complexes, such as b-TrCP-SKP1-CUL1-RBX1, downregulate NRF2, so it is maintained at a low level in healthy cells [22,23]. Oxidative stress leads to Protein kinase C (PKC)-mediated phosphorylation of NRF2 at S40 and AMPK-mediated phosphorylation of NRF2 at S550, and this triggers its nuclear translocation [24,25]. At the transcriptional level, the oncogenes $KRas^{G12D}$, $Braf^{V619E}$, and Myc^{ERT2} each increase NRF2 expression, and this increases antioxidant activity [15].

SUMOylation is a process in which small ubiquitin-like proteins (SUMOs) are added to a protein [28–30] and thereby modifies protein activity. In particular, previous research reported that SUMO-specific protease 1 (SNEP1) de-SUMOylates NRF2 [26,27]. However, the biological significance of NRF2 SUMOylation in cancers remains largely unknown. The purpose of this study was to examine the role of NRF2 SUMOylation on *de novo* serine synthesis and HCC tumorigenesis. We found that NRF2 was modified at the conserved site lysine 110 (K110), and this modification maintained tumorigenesis of HCC *in vitro* and *in vivo*. Mechanistically, NRF2 SUMOylation promotes the clearance of intracellular ROS by increasing the transcription of glutathione peroxidase 2 (*Gpx2*), and this leads to upregulation of PHGDH in HCC cells. These changes promote *de novo* serine synthesis and the production of one-carbon units for the synthesis of purines, thereby promoting HCC. Indeed, our LC-MS analyses indicated that NRF2 SUMOylation deficiency reduced the accumulation of serine and purines in HCC. More importantly, serine starvation increased NRF2 SUMOylation, thus maintaining HCC growth in response to this metabolic stress. Taken together, our study identified a novel signal transduction pathway in which NRF2 SUMOylation promoted *de novo* serine synthesis and maintained HCC tumorigenesis.

2. Materials and methods

2.1. Plasmids, antibodies, and reagents

pcDNA3-Myc3-NRF2 was purchased from Addgene (#21555). Flag-NRF2 and Flag-NRF2 mutants (K110R, K533R, K603R, K533/603R, K53R, K56R, K64R, K68R, K389R, K394R, K438R, K518R, K543R, K599R) were generated using standard cloning procedures and site-directed mutagenesis with the Quick Change kit from Stratagene. The antibodies, concentrations, and sources were as follows: FLAG (Sigma; 1:2000), β-ACTIN (Cell Signaling Technology; 1:2000), Lamin B (Santa Cruz Biotechnology; 1:2000), NRF2 (abcam; 1:3000 for Western blots and 1:400 for immunoprecipitation [IP]), PHGDH (Sigma; 1:250), PSPH (Gene Tex; 1:3000). Menadione sodium bisulfite (MENA) and cycloheximide (CHX) were from Sigma, and carboxy-H2DCFDA was from Invitrogen (Gaithersburg, MD, USA).

2.2. Cell culture and treatments

HEK293T cells, SMMC-7721, and HepG2 cells were cultured in DMEM (Hyclone) containing 10% v/v fetal bovine serum (Gibco), 1% penicillin, and 1% streptomycin in a 37 °C incubator with 5% CO_2. For MENA experiments, SMMC-7721 cells were grown to 80% confluence in 6-well plates, and then treated with 25 μM MENA for 12 h. For serine starvation experiments, cells were cultured for 72 h in DMEM that lacked serine and glycine (Shanghai Basalmedia Technology), but that had fetal bovine serum (Gibco), penicillin, and streptomycin.

2.3. Ni^2-NTA agarose bead pull-down assay

NRF2 SUMOylation was analyzed in HEK293T cells using an *in vivo* SUMOylation assay with Ni^{2+}-NTA agarose beads. Flag-NRF2-, His-SUMO1-, and HA-UBC9-expressing plasmids were used to transfect HEK293T cells with Lipofectamine™ 2000 (Invitrogen) according to the manufacturer's instructions. At 24 h after transfection, cells were collected. A total of 10% of these cells were used for Western blot analysis; the other cells were lysed in 1 mL of His-lysis buffer (6 M guanidinium-HCl, 0.1 M Na_2HPO_4/NaH_2PO_4, 0.01 M Tris/HCl, pH 8.0, 5 mM imidazole, and 10 mM β-mercaptoethanol) and then added to 20 μL of Ni^{2+}-NTA agarose beads (Qiagen), and maintained on a shaker at 4 °C overnight. The beads were successively washed (15 min per step) at room temperature with 1 mL in each of the following buffers: washing buffer-1 (6 M guanidinium-HCl, 0.1 M Na_2HPO_4/NaH_2PO_4, 0.01 M Tris/HCl, pH 8.0, 10 mM β-mercaptoethanol); washing buffer-2 (8 M urea, 0.1 M Na_2HPO4/NaH_2PO4, 0.01 M Tris/HCl, pH 8.0, 10 mM β-mercaptoethanol); washing buffer-3 (buffer 1 with 0.2% Triton X-100); and washing buffer 4 (buffer 1 with 0.1% Triton X-100). Finally, the beads were incubated in 60 μL of elution buffer (200 mM imidazole, 0.15 M Tris/HCl pH 6.7, 30% glycerol, 0.72 M β-mercaptoethanol, 5% SDS) for 30 min at room temperature. The eluates were analyzed by western blotting.

2.4. Western blotting

Cells were washed with cold PBS and lysed in RIPA lysis buffer that was supplemented with protease and phosphatase inhibitors on ice for 20 min. The lysates were centrifuged at 13,000 rpm for 15 min at 4 °C, and the supernatants were collected. Total protein was resolved in 10% SDS/PAGE gels, followed by electrophoretic transfer to PVDF membranes in a Tris-glycine buffer. The membranes were blocked at room temperature for 1 h in 5% non-fat milk with TBS-Tween (TBST) on a shaker, and then incubated with the primary antibodies overnight at 4 °C. The membranes were washed in TBST at least 5 times (5 min each) and then incubated with HRP conjugated anti-rabbit or anti-mouse IgG at room temperature for 1 h with gentle shaking. The ECL substrate was added, and the results were visualized using ImageQuant LAS 4000 (GE). β-actin was used as loading control, and optical density quantified using ImageJ software. Each experiment was repeated three times.

2.5. Plate colony formation

SMMC-7721 cells (400 per well) were added to 6-well plates, and the medium was replaced every 3 days. After 2–4 weeks, images of the colonies were recorded using scanner (Epson Perfection V800 Photo) and the colonies were counted using Image J software.

2.6. Tumor xenograft assay

Five-week old female nude mice were purchased from Shanghai Ling Chang Biotechnology. For tumor xenograft experiments, each mouse received a single subcutaneous injection of 1×10^6 SSMC-7721 cells with stable overexpression of NRF2, K110R cells, or vector control cells (5 per group). Tumor volume (mm^3) was calculated every 4 days from caliper measurements using formula $(L + W^2)/2$, where L is the length (long-axis) and W is the width (short-axis). Seventeen days after injection, mice were killed and tumor weight was measured. None of the tumors exceeded the limit for tumor burden (10% of total body weight or 2 cm in diameter). All animal experiments were carried out according to the institutional guidelines of Shanghai Jiaotong University School of Medicine.

2.7. Measurement of intracellular ROS

Cells were harvested by trypsin digestion, washed with PBS, and incubated with Carboxy-H2DCFDA (DCF; Invitrogen; final concentration of 10 μM) in DMEM medium for 30 min at 37 °C. Then, cells were washed three times with cold PBS and intracellular ROS was measured using the BD FACS Aria Flow Cytometer (Becton Dickinson, Franklin Lake, NJ). For measurement of DCF fluorescence, the excitation wavelength was 488 nm and the emission wavelength was 525 nm.

2.8. Measurement of GSH and GSSG

The levels of total glutathione (GSH) and oxidized glutathione (GSSG) were measured using a GSH and GSSG Assay Kit (S0053, Beyotime), according to manufacturer's instruction. The GSH/GSSG ratio was then calculated from these data.

2.9. Quantitative real-time PCR

Total RNA was isolated using the Trizol reagent (Invitrogen). Total RNA (1 μg) was then used to synthesize complementary DNA (cDNA) using a cDNA synthesis kit (Takara) according to the manufacturer's instructions. Further analysis was performed with SYBR Premix ExTaq (Takara) using the LightCycler 480IIsystem (Roche). Expression was normalized to the level of 18S rRNA in the same samples. Each sample was analyzed in triplicate, and experiments were performed three times. Table S1 shows the PCR primers used for amplification.

2.10. Chromatin immunoprecipitation assay

Formaldehyde cross-linked chromatin was prepared from SSMC-7721 cells, and immunoprecipitation was performed using the Chromatin Immunoprecipitation (ChIP) Assay Kit according to the manufacturer's protocol (Upstate Biotechnology). Briefly, cells were cross linked with 1% formaldehyde for 10 min at room temperature, and then neutralized by addition of glycine (final concentration of 0.125 M). Cells were then washed twice with cold PBS and then harvested and suspended in cold cell lysis buffer containing protease inhibitors. After 15 min at 4 °C, nuclei were harvested and re-suspended in a nuclear lysis buffer. After sonication, the supernatants were added to magnetic beads, and specific antibodies (or IgG control) and incubated overnight at 4 °C. Beads were washed sequentially in four buffers (low-salt wash buffer, high-salt wash buffer, LiCl wash buffer, and TE buffer). After reverse cross-linking for 6 h at 62 °C, DNA was extracted and quantitative PCR was performed using the primers in Table S1.

2.11. Oxygen consumption rate and extracellular acidification rate

The intact cellular oxygen consumption rate (OCR) and extracellular acidification rate (ECAR) of SSMC-7721 cells were measured using the Seahorse XF Cell Mito Stress Test and the Seahorse XF-96 Extracellular Flux Analyzer (Seahorse Bioscience, Agilent Technologies, Waldbronn, Germany). First, 3×10^4 cells (SSMC-7721-Vector, SSMC-7721-NRF2, or SSMC-7721-K110R) were seeded into 96-well Seahorse microplates in 80 μL of growth medium and incubated at 37 °C in 5% CO_2 for 24 h. The calibrator plate was equilibrated in an incubator without CO_2 overnight. The analyzer determined the OCR and corresponding ECAR following three sequential additions: oligomycin (1 μM), an inhibitor of ATP synthase which leads to maximal glycolysis; carbonyl cyanide-4 (trifluoromethoxy) phenylhydrazone (FCCP) (0.25 μM), an uncoupler of the electron transfer chain (ETC) and inhibitor of oxidative phosphorylation which induces peak oxygen consumption (an indirect measure of maximal oxidative metabolism); and then rotenone (0.5 μM; which inhibits the ETC) and antimycin A (0.5 μM; which inhibits complex III). These experiments allowed calculation of basal respiration, maximal respiration, and ATP production. The BCA Protein Assay Kit (Beyotime, China) was used according to the manufacturer's instructions to determine the protein concentration for normalization of OCR and ECAR. These data were analyzed and visualized using wave software (Version 2.3.0, Seahorse Bioscience, Agilent Technologies, Waldbronn, Germany).

2.12. High-performance liquid chromatography-mass spectrometry

HPLC-MS experiments were performed in the Core Facility of Basic Medical Sciences, College of Basic Medical Sciences, Shanghai Jiao Tong University School of Medicine. For metabolite extraction, cells were harvested and re-suspended in a solution of HPLC-grade acetonitrile, methanol, and water (2/2/1 by volume) that was supplemented with internal standards. Chromatographic analyses were performed using the Dionex UltiMate 3000 HPLC System (Thermo Scientific) with the Thermo Hypersil Gold (2.1 mm × 100 mm, 1.9 μm) analytical column. The injection volume was 5 μL, and the temperature of the column was maintained at 40 °C. The mobile phases were H_2O + 0.1% formic acid (mobile phase A) and ACN + 0.1% formic acid (mobile phase B), and the flow rate was 0.3 mL/min. The total chromatographic run time was 11 min.

A triple quadrupole mass spectrometer (TSQ Vantage, Thermo Scientific) was used for mass analysis and quantification of target analytes. The MS was operated in positive ion mode with selected reaction monitoring (SRM). The tuning parameters were optimized for the target analytes. The sheath and auxiliary gas was nitrogen, the spray voltage was 3000 V, the vaporizer temperature was 300 °C, the sheath gas pressure was 40 psi, the auxiliary gas pressure was 10 psi, and the capillary temperature was 320 °C.

2.13. Endogenous NRF2 SUMOylation assay

Immunoprecipitation was used to measure endogenously SUMOylated-NRF2. Briefly, 1×10^7 cells were added to 500 μL of lysis buffer (50 mM sodium phosphate, pH 7.4, 400 mM NaCl, 0.1% SDS, 1% Triton, 10 mM N-ethylmaleimide [NEM], protease inhibitors, phosphatase inhibitors). The viscous lysate was sonicated until it became fluid, and 10% of the cells were used; the remaining cells were incubated with antibody overnight at 4 °C. Beads were washed three times with lysis buffer, boiled for 10 min in SDS sample buffer, and then subjected to Western blot analysis.

2.14. 5-Bromodeoxyuridine assay

For the BrdU assay, 10,500 cells per well were seeded into each well of 96-well plates, labeled with BrdU (10 μM) for 4 h, and then subjected to fixation. The incorporated BrdU was detected by immunostaining, with measurement by a microplate spectrophotometer at 450 nm. Cell proliferation rate was determined using the BrdU cell proliferation assay kit according to the manufacturer's instructions (Cell Signaling Technology). Measurements were performed at 0, 12, 24, 48, and 72 h.

2.15. Statistical analysis

The statistical significance of differences between two groups was evaluated using the two-tailed Student's *t*-test. Statistical significance is expressed as * ($P < 0.05$), ** ($P < 0.01$), or *** ($P < 0.001$). All values are presented as means ± SDs. Data analyses were performed using GraphPad Prism (Version 6).

3. Results

3.1. SUMO1 conjugates human NRF2 at K110

Our Ni^{2+} NTA agarose pull-down assay and immunoblotting

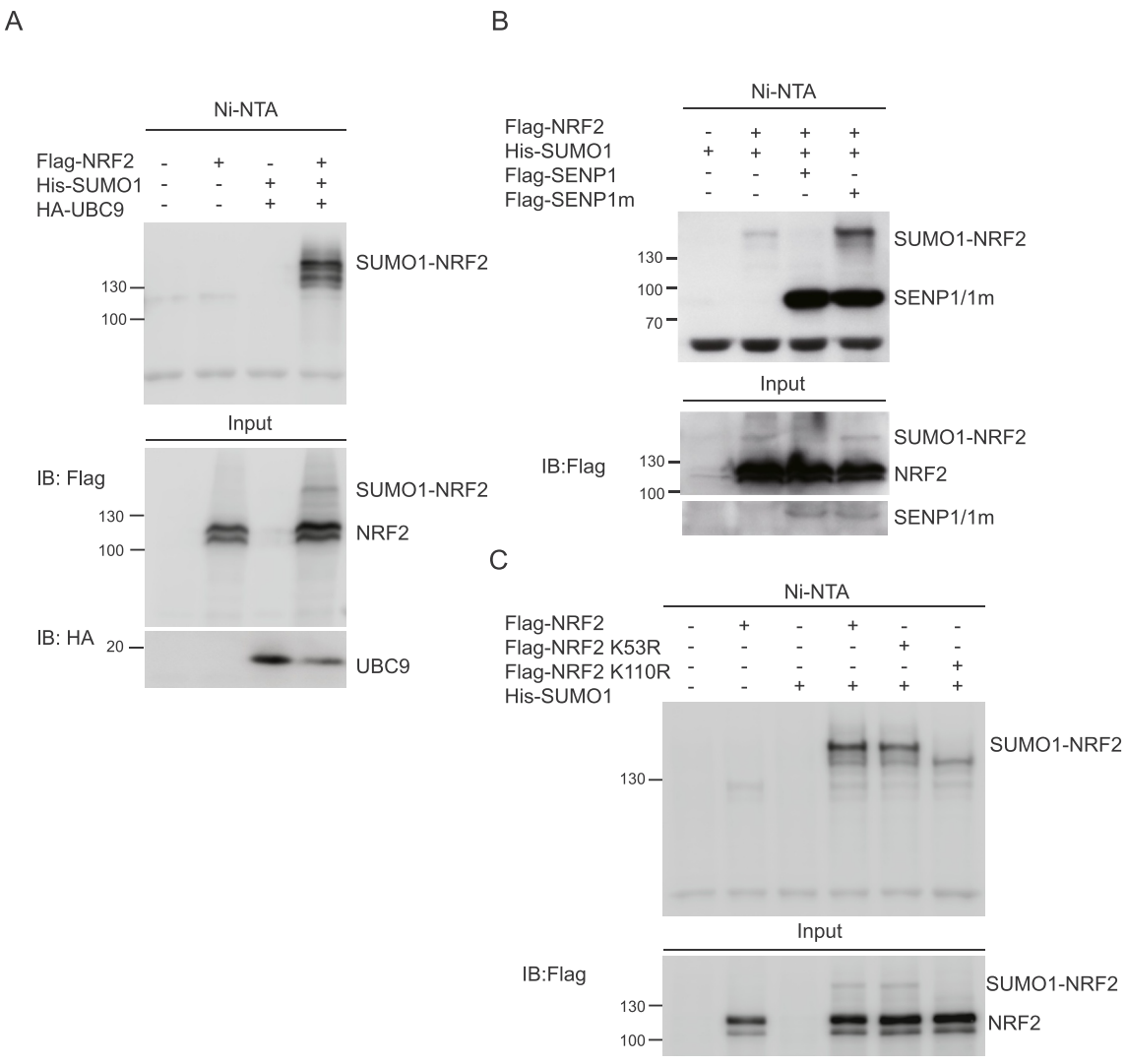

Fig. 1. SUMO1 conjugates human NRF2 at K110. **A**, HEK293T cells were transfected with Flag-NRF2 with or without His-SUMO1 and HA-Ubc 9. SUMOylated proteins were purified from cell lysates using Ni2 + -NTA agarose bead pull-down, and SUMOylated NRF2 was detected by immunoblotting with an anti-Flag antibody. **B**, His-SUMO1-conjugated proteins were purified by Ni2 + -NTA agarose bead pull-down from HEK293T cells expressing Flag-NRF2 and His-SUMO1 by use of SENP1 or SENP1m, and probed with Flag. **C**, HEK293T cells were co-transfected with Flag-NRF2 wild-type or Flag-NRF2 mutants with or without His-SUMO1.

experiments confirmed that SUMO1 conjugates NRF2 (Fig. 1A). In addition, wild-type (WT) SENP1 deconjugated the SUMO1 modification of NRF2, but the catalytic mutant (SENP1m) did not (Fig. 1B).

Although the SUMOylation sites in NRF2 are uncertain, Malloy et al. [26] predicted SUMOylation sites at K533 and K603 (Fig. S1A). Thus, we evaluated these two sites by mutating each lysine (K) to arginine (R). The single- or double-lysine mutation of these two sites did not change the SUMOylation of NRF2 in transfected cells (Fig. S1B). Based on other potential SUMOylation sites predicted by SUMOplot™ (http://www.abgent.com/sumoplot) and JASSA (http://www.jassa.fr), we individually mutated K53, K56, K64, K68, K110, K389, K394, K438, K518, K543, or K599 into arginine (R) in NRF2 in transfected cells (Figs. S2A and S2B). The results indicated that only the K110 mutation decreased SUMOylation (Fig. 1C and Fig. S2C). These data thus indicate that SUMO1 conjugates human NRF2 at the K110 residue, which is conserved in humans, mice, and rats (Fig. S3).

3.2. NRF2 SUMOylation maintains HCC tumorigenesis

We next characterized the role of NRF2 K110 SUMOylation in tumors by establishing three lines of HCC cells, each with knock-down of endogenous NRF2 expression: one line expressed vector alone (SSMC-7721-Vector); the second line expressed NRF2 WT (SSMC-7721-NRF2); and the third line expressed NRF2 K110R (SSMC-7721-NRF2 K110R) (Fig. S4). The results indicated that SUMOylation of NRF2 was significantly attenuated in SSMC-7721-NRF2 K110R cells (Fig. S4C).

A plate-colony formation assay showed that NRF2 SUMOylation significantly promoted cell colony formation (Fig. 2A, $p < 0.01$). In addition, a deficiency in NRF2 SUMOylation significantly impaired colony formation in HepG2 cells and in two lines of NSCLC cells (H1299 and A549; Fig. S5). In addition, as shown in Fig. S6, we found that NRF2 SUMOylation did not significantly affect the *in vitro* apoptosis of SMMC-7721 cells. Then, we analyzed the effect of SUMOylation on tumorigenesis *in vivo* by implanting SSMC-7721 cells into nude mice and measurement of tumor weight after 17 days. The results show that tumors from SMMC-7721-NRF2 cells were significantly larger than those from SMMC-7721-Vector cells (Fig. 2B–D; $p < 0.01$), and the tumors from SMMC-7721-NRF2 K110R cells were intermediate in size. These *in vitro* and *in vivo* data thus suggest that NRF2 SUMOylation may function in maintaining HCC tumorigenesis, although this mutation could potentially interfere with other functions of NRF2.

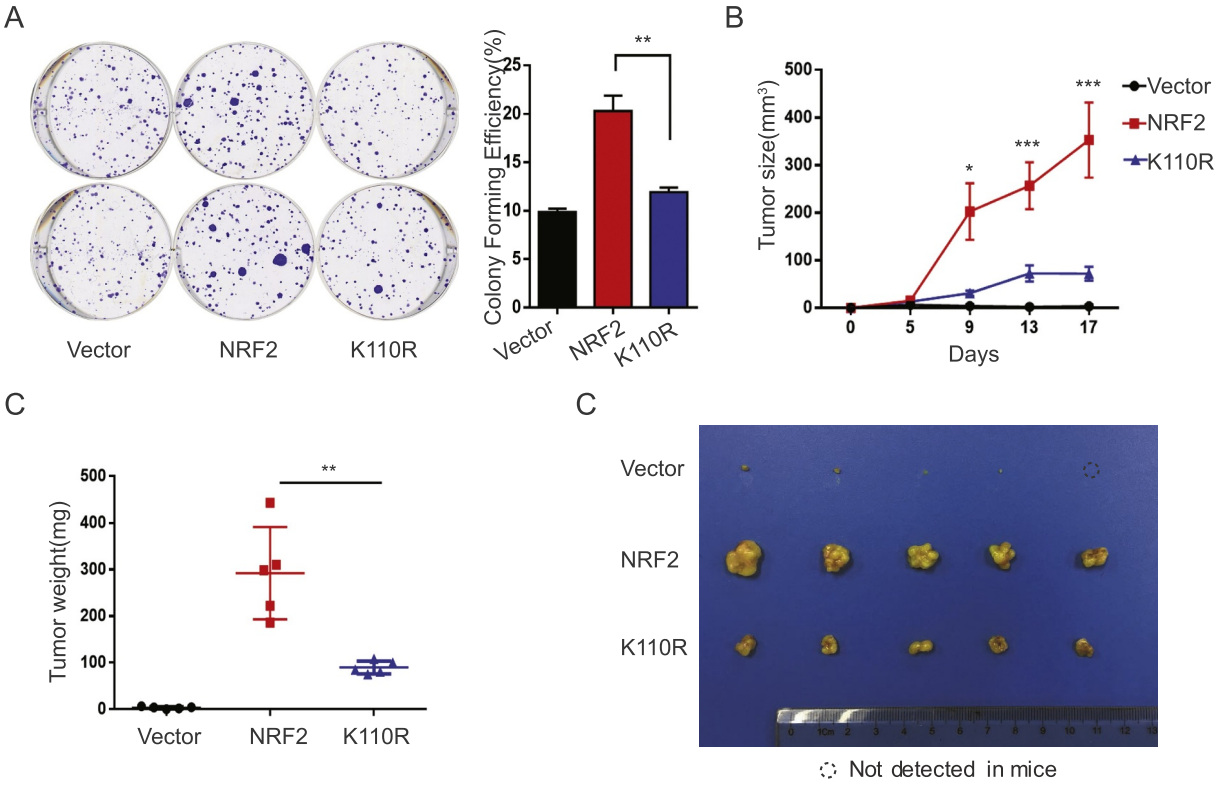

Fig. 2. NRF2 SUMOylation maintains HCC tumorigenesis. **A**, Cells containing SSMC-7721-Vector, SSMC-7721-NRF2, or SSMC-7721-NRF2 K110R were plated in 6-well plates and stained with crystal violet. Images of the colonies were taken using a scanner and colonies were counted (3 replicates per group). **B**, Five-week old mice were used to establish tumor xenografts using subcutaneous injections of 1 × 106 SSMC-7721 cells stably overexpressing NRF2, K110R, or vector controls (5 mice per group). Tumor volumes were calculated by caliper measurements. **C**, Seventeen days after injection, mice were killed and tumor weight was determined. **D**, Representative subcutaneous tumors isolated from mice that received SSMC-7721-Vector, SSMC-7721-NRF2, or SSM-7721-NRF2 K110R cells.

3.3. NRF2 SUMOylation decreases intracellular ROS level in HCC by activating Gpx2 transcription

NRF2 attenuates oxidative stress by induction of genes that quench ROS. Our results indicated that SSMC-7721-NRF2 cells had lower levels of intracellular ROS than SSMC-7721-Vector cells and SSMC-7721-NRF2 K110R cells (Fig. 3A). Consistently, SSMC-7721-NRF2 cells had a greater GSH/GSSG ratio than SSMC-7721-NRF2 K110R cells (Fig. 3B, $p < 0.05$). In addition, NRF2 upregulated the expression of genes encoding key components of the GSH-dependent antioxidant system (Fig. 3C).

We further examined whether NRF2 SUMOylation reduced cellular ROS level through transcriptional upregulation of these target genes by performing using real-time PCR to analyze the transcription of genes involved in GSH synthesis and ROS scavenging (Fig. 3D). The results indicated that NRF2 SUMOylation functioned as an antioxidant chiefly by upregulating the transcription of *Gclc*, *Gclm* and *Gpx2*. GPX2 is a protein with peroxidase activity. There was also a significantly greater level of *Gpx2* in HCC tumor samples from nude mice injected SSMC-7721-NRF2 rather than SSMC-7721-NRF2 K110R cells (Fig. 3E, $p < 0.05$).

We used a ChIP assay to further examine the possible mechanism of this effect. The results indicated that SUMOylation of NRF2 led to binding to the *Gpx2* promoter and recruitment of the coactivator protein, chromodomain-helicase-DNA-binding protein 6 (CHD6), which activated transcription (Fig. 3F). There were no significant differences between NRF2 WT and NRF2 K110R proteins in binding with KEAP1, ubiquitination, and their stability in the cells (Figs. S7A–7C).

3.4. Reduced ROS level in HCC cells increases PHGDH expression

NRF2 regulates serine metabolism by activating the expression of enzymes that control *de novo* serine synthesis from glucose (Fig. 4a), indirectly through transcription factor ATF4 [6]. Our real-time PCR analyses of HCC cells indicated that NRF2 SUMOylation had no impact on transcription of genes encoding enzymes that catalyze *de novo* serine synthesis (Fig. 4b). However, analysis of proteins indicated elevated levels of PHGDH, PSAT1, and PSPH in SSMC-7721-NRF2 cells relative to SSMC-7721-Vector and SSMC-7721-NRF2 K110R cells (Fig. 4c). Consistent with these *in vitro* results, mice injected with SSMC-7721-NRF2 cells had greater tumor levels of PHGDH than mice injected with SMMC-7721-NRF2 K110R cells (Fig. 4d, $p < 0.001$).

The control of redox homeostasis by NRF2 can prevent cysteine oxidation of proteins involved in mRNA translation, thereby supporting protein translation [31]. In agreement, we found that addition of the oxidant MENA to SMMC-7721-NRF2 cells increased the intracellular ROS level, and reduced the level of PHGDH (Fig. 4e and Fig. S8). These results suggest that the effect of NRF2 SUMOylation on PHGDH translation is at least partially ROS-dependent.

3.5. Increased PHGDH expression leads to accumulation of serine and nucleotides in HCC cells

The serine biosynthetic pathway is an important source of metabolic intermediates that support the rapid proliferation of cancer cells. To investigate whether alterations in the expression of PHGDH was associated with changes in the metabolism in HCC cells, we measured the levels of multiple metabolites (3-phophoserine [3-PS], serine, AMP, GMP, adenine, and guanine) using HPLC-MS (Table S2). The results indicated that SSMC-7721-NRF2 cells accumulated more serine

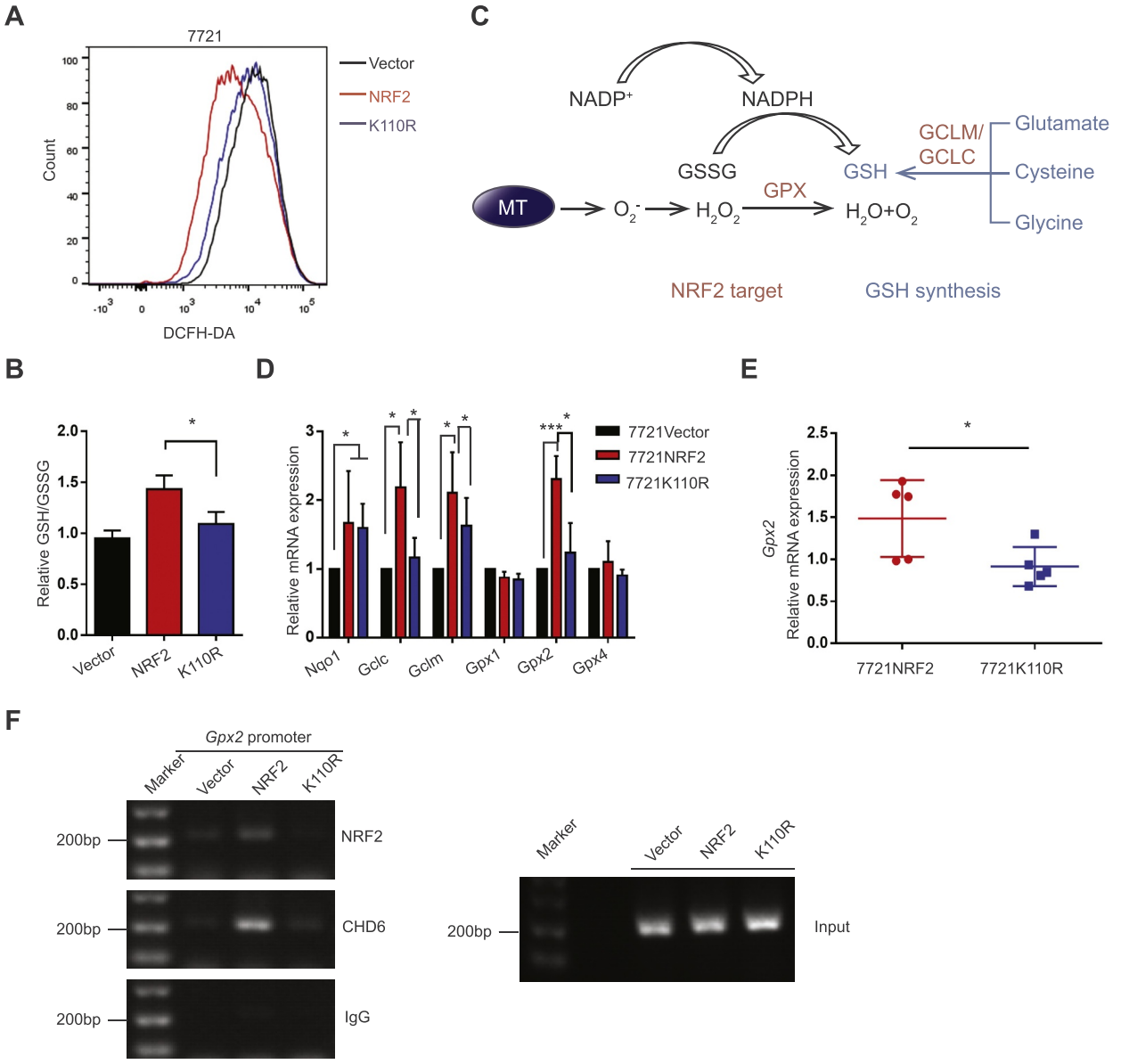

Fig. 3. NRF2 SUMOylation decreases intracellular ROS level in HCC by increasing *Gpx2* transcription. **A**, The three cells types were incubated with Carboxy-H2DCFDA (final concentration: 10 μM) in DMEM for 30 min at 37 °C. Cells were then washed and intracellular ROS was measured. **B**, Levels of total glutathione (GSH + GSSG), oxidized glutathione (GSSG), and the GSH/GSSG ratio in the different groups (3 replicates per group). **C**, Enzymes regulated by Nrf2 during GSH metabolism. **D**, Real-time PCR of genes involved in GSH metabolism that are targeted by NRF2 (3 replicates per group). **E**, Real-time PCR of *Gpx2* in tumor tissues of mice injected with SSMC-7721-NRF2 or SSMC-7721-NRF2 K110R cells (5 replicates per group). **F**, ChIP assay with anti-NRF2 or anti-CHD6 antibody was conducted in the three cell types. RT-PCR was used to amplify the promoter of *Gpx2*. *Gclc*, glutamate-cysteine ligase, catalytic subunit; *Gclm*, glutamate-cysteine ligase, modifier subunit; *Gpx*, glutathione peroxidase.

($p < 0.01$) and purines ($p < 0.001$) than SSMC-7721-Vector cells (Fig. 5d and e). However, NRF2 SUMOylation almost completely blocked *de novo* serine synthesis (Fig. 5d and e and). Consistent with these metabolite changes, measurement of ECAR indicated that the rate of glycolysis was significantly increased in SSMC-7721-NRF2 (Fig. 5a, $p < 0.001$), whereas the OCR and ATP production were similar in SSMC-7721-NRF2 and SSMC-7721-NRF2 K110R cells (Fig. 5b and c). These results indicate that SSMC-7721-NRF2 cells have an increased rate of glycolysis, and this provides them with more of the metabolites needed to support cell proliferation (Fig. 4a).

3.6. NRF2 SUMOylation increases HCC cell resistance to serine starvation

Taken together, the results above suggest that NRF2 SUMOylation is required for *de novo* serine synthesis in HCC. We next examined the effect of limiting the level of exogenous serine on cell proliferation and tumorigenesis. Thus, we measured the proliferation of SSMC-7721 cells using a BrdU assay with or without serine in the culture media. The results indicated that under normal conditions, there were no significant differences in the number of cells in the SMMC-7721-NRF2 and SMMC-7721-NRF2 K110R groups (Fig. 6a). However, upon serine starvation, SMMC-7721-NRF2 K110R cells had a slower proliferation rate than SMMC-7721-NRF2 cells (Fig. 6a). Furthermore, serine starvation induced NRF2 SUMOylation in SSMC-7721-NRF2 cells (Fig. 6b), suggesting that this has a role in signaling serine starvation. The increased NRF2 SUMOylation in HCC cells might be attributable to the down-regulation of SENP1 (Fig. S9).

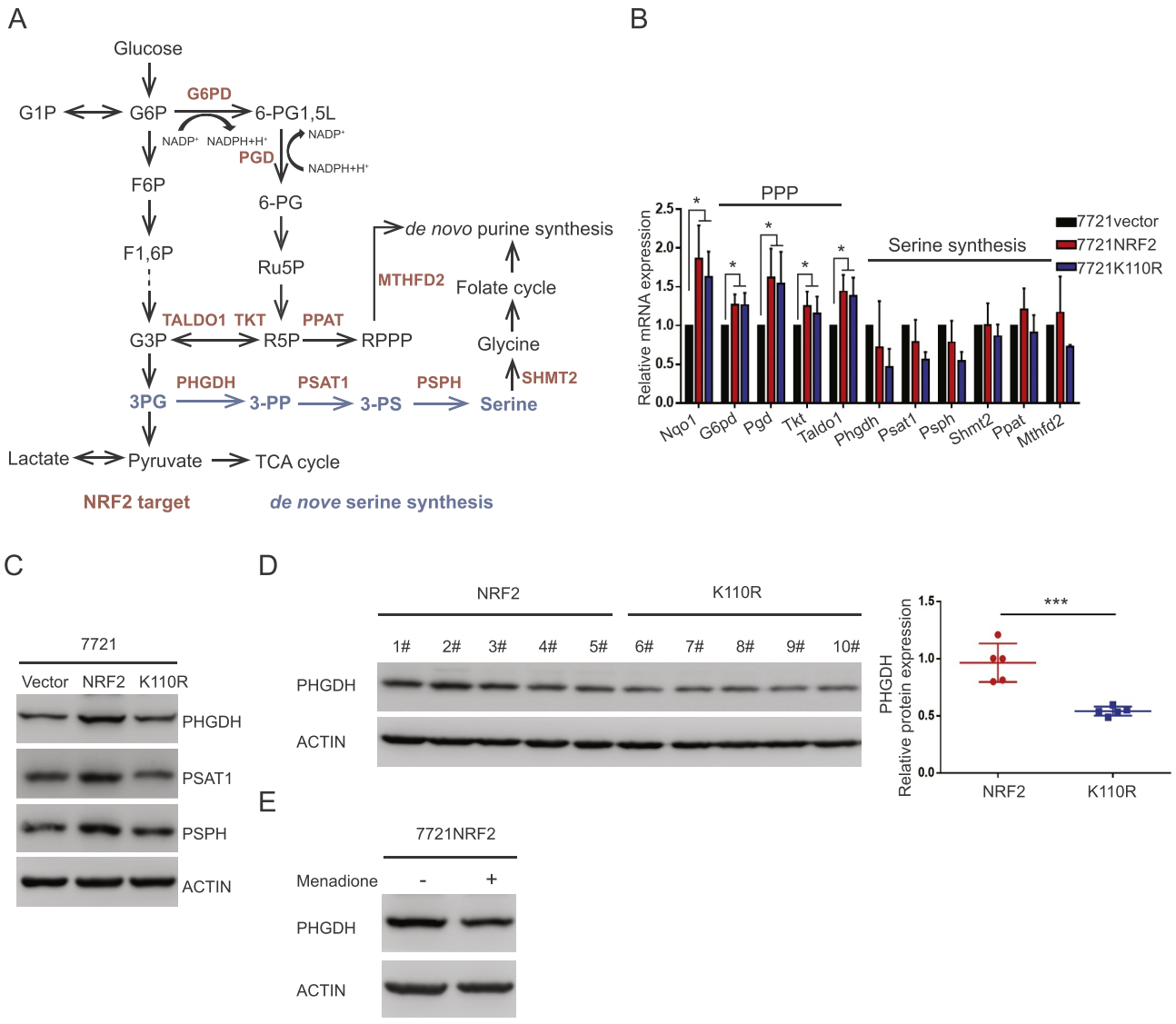

Fig. 4. SMMC-7721-NRF2 cells reduce ROS levels and upregulate PHGDH expression. **A**, Enzymes in the pentose phosphate pathway regulated by NFR2 and *de novo* serine synthesis pathway. **B**, Expression of *Nrf2* target mRNAs in the pentose phosphate pathway and *de novo* serine synthesis pathway were analyzed by real-time PCR in the three cell types (3 replicates per group). **C**, Western blotting of PHGDH, PSAT1, and PSPH in the three cell types. **D**, Western blotting of PHGDH in tumor tissues from. mice injected with SSMC-7721-Nrf2 or SSMC-7721-Nrf2 K110R cells (5 replicates per group). **E**, SMMC-7721 cells were treated with 25 μM MENA for 12 h, and the PHGDH was measured by western blotting and intracellular ROS was measured by FACS. *G6pd*, glucose-6-phosphate dehydrogenase; *Pgd*, 6-Phosphogluconate dehydrogenase; *Tkt*, transketolase; *Taldo1*, transaldolase; *Phgdh*, phosphoglycerate dehydrogenase; *Psat1*, phosphoserine aminotransferase; *Psph*, phosphoserine phosphatase; *Shmt2*, serine hydroxymethyltransferase; *Ppat*, phosphoribosylpyrophosphate amidotransferase; *Mthfd2*, methylenetetrahydrofolate dehydrogenase; MENA, menadione.

4. Discussion

In this study, we first identified the conserved lysine 110 in human NRF2 as the SUMO1 conjugation site (Fig. 1C). No previous studies have identified acceptor sites of Nrf2 K110 for any type of post-translational modification.

(https://www.phosphosite.org/proteinAction.action?id=3828&showAllSites=true). K110 is located in Neh4 domain (Nrf2-ECH homology domain 4) of NRF2, one of the transactivation domains essential for regulating transcriptional activity. Ramani et al. reported that SUMO1 conjugation of NRF2 enhanced its binding to the target gene during hepatic fibrogenesis of activated hepatic stellate cells [27]. The same group examined hepatocytes and macrophages and reported that reduced SUMO1 modification of NRF2 led to reduced expression of glutamate-cysteine ligase (*GCL*) following treatment with lipopolysaccharide (LPS) [32]. Previous research reported that SUMO1 modification is required for the interaction of NRF2 with MafG, ARE binding, and *GCLC* expression [27]. Consistent with these findings, our study of HCC cells indicated that NRF2 K110 SUMOylation enhanced *Gclc* and *Gclm* transcription (Fig. 3D). We also found that SUMO1 modification promoted the binding of NRF2 to the *Gpx2* promoter in HCC cells (Fig. 3F), leading to recruitment of the transcription coactivator CHD6, and increased *Gpx2* transcription. GCLC and GCLM catalyze the synthesis of GSH, which is dependent on GPX2 for reducing the oxidative insults in cells. However, our NRF2 WT and K110R cells had no differences in the transcription of thioredoxin-dependent antioxidant systems (data not shown). This cell-type specific and context-dependent transcriptional regulation by NRF2 K110 SUMOylation requires future investigation.

Our results indicated that NRF2 SUMOylation maintains HCC tumorigenesis *in vitro* and *in vivo* (Fig. 2). Our examination of the underlying mechanism indicated that NRF2 K110 SUMOylation promoted

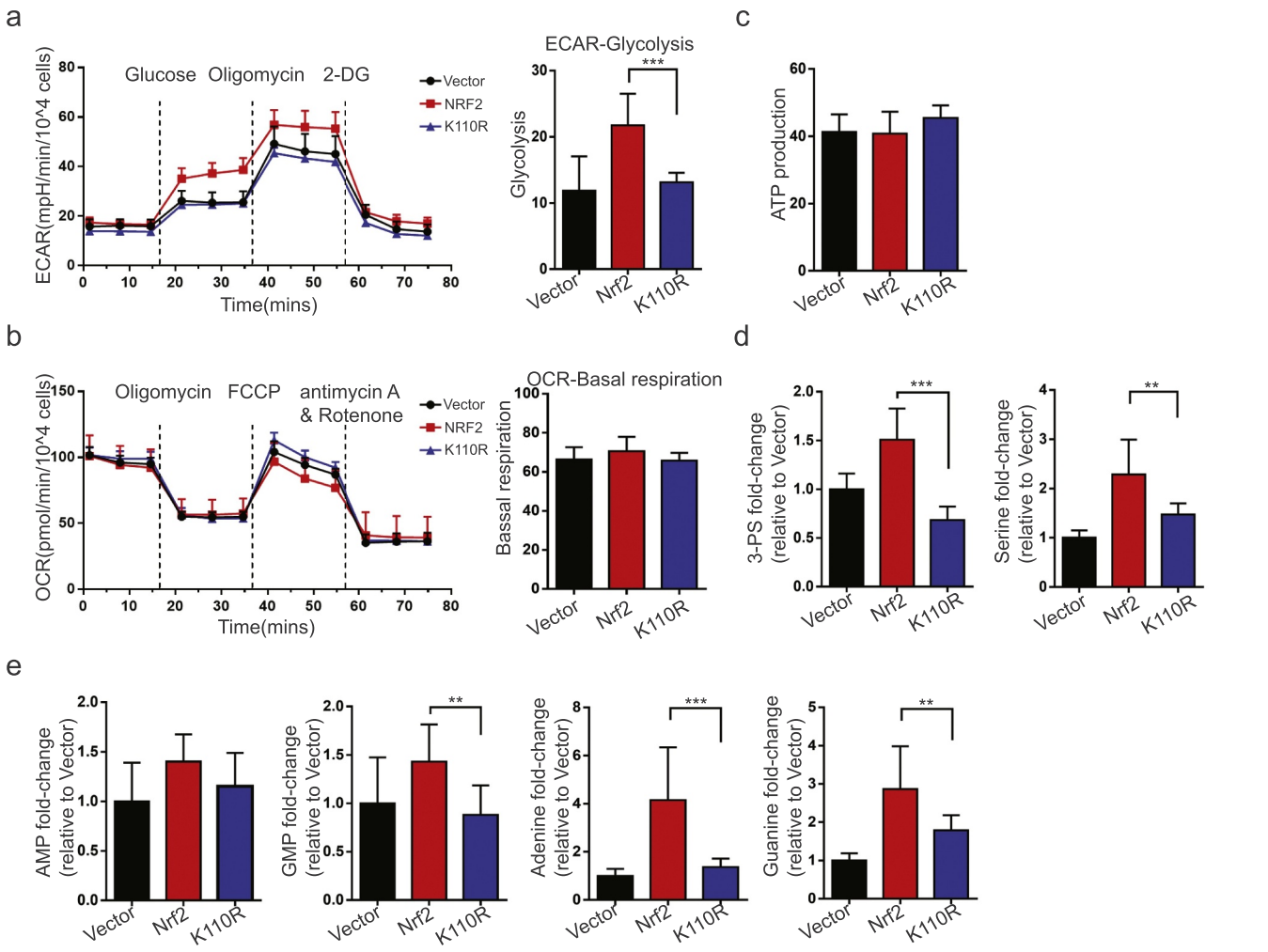

Fig. 5. Increased PHGDH expression leads to accumulation of serine and nucleotides in SSMC-7721-NRF2 cells. **A**, The three cell types were treated with glucose, oligomycin, and 2-deoxy-D-glucose (2DG) as indicated, and changes in ECAR were determined (3 replicates per group). **B**, OCR in the three cell types in response to oligomycin, FCCP, and rotenone (3 replicates per group). **C**, ATP levels in the three cell types (3 replicates per group). **D**, Levels of metabolic intermediates in the *de novo* serine synthesis pathway, from. HPLC-MS (10 replicates per group). **E**, Levels of metabolic intermediates in purine metabolism, from HPLC-MS (10 replicates per group).

ROS scavenging *via* transcriptional activation of *GPX2* in HCC cells, and that this protected HCC cells from oxidative stress. However, NRF2 has additional functions in cancer beyond its redox-regulating capacities [2,33–36]. In particular, although NRF2 activates the transcription of enzymes involved in redox regulation [6], NRF2 SUMOylation up-regulates SSP at the translational level (Fig. 4). NRF2 also has an indirect effects through its redox modulation of target genes [31,37]. For example, in pancreatic cancer NRF2 stimulates mRNA translation by inhibiting the oxidation of specific translational regulatory factors [31]. Bar-Peled et al. found that proteins which have cysteines that undergo specific reactivity changes in shNRF2 NSCLC cells are mainly in pathways that include protein translation (EEF2) and protein folding (PDIA3) [37]. These two studies [31,37] thus established that NRF2 has an indirect effect in modulation of protein translation. Serine is a non-essential amino acid and an important building-block in protein translation. Because NRF2-regulated ROS homeostasis indirectly controls protein translation, the same mechanism may also regulate serine biosynthesis. PHGDH, PSAT1, and PSPH are the key enzymes that catalyze serine synthesis from glucose (Fig. 4A). Our results showed for the first time that the NRF2 SUMOylation-regulated homeostasis of ROS in HCC affects the level of PHGDH in these cells (Fig. 4C–E).

PHGDH diverts glycolytic flux and promotes serine and glycine biosynthesis in many tumor types [38]. A recent study reported that PHGDH defines a metabolic subtype of lung adenocarcinoma with poor prognosis [39]. In agreement, HCC patients with up-regulation of PHGDH have accelerated tumor development because of metabolic diversion from glycolysis to serine biosynthesis [40]. Pacold et al. demonstrated that PHGDH inhibition reduced the incorporation of one-carbon units (from glucose-derived serine) into nucleotides [38]. Our results are consistent with these previous results, in that an increased level of PHGDH in SSMC-7721-NRF2 cells was associated with their higher rate of glycolysis (Fig. 5A). Thus, NRF2 SUMOylation may promote glucose flux toward serine biosynthesis. Indeed, our MS analyses showed accumulation of 3-PS, serine, and purines in SSMC-7721-NRF2 cells (Fig. 5D and E). These results suggest that the NRF2 SUMOylation-mediated regulation of PHGDH translation and promotion of serine and nucleotide biosynthesis helps to maintain HCC tumorigenesis, in addition to facilitating the transcription of ROS scavenging proteins.

There are multiple mechanisms by which cancers stimulate NRF2 function upon stress [3]. Our results showed that serine starvation caused HCC cells to up-regulate NRF2 SUMOylation as a defense against oxidative-stress, thereby maintaining HCC growth (Fig. 6A and B). Upon amino acid starvation, eIF2 kinase and GCN2 repress the translation of most mRNAs, but they selectively increase the translation of activating transcription factor 4 (ATF4) [41,42]. The GCN2-eIF2-

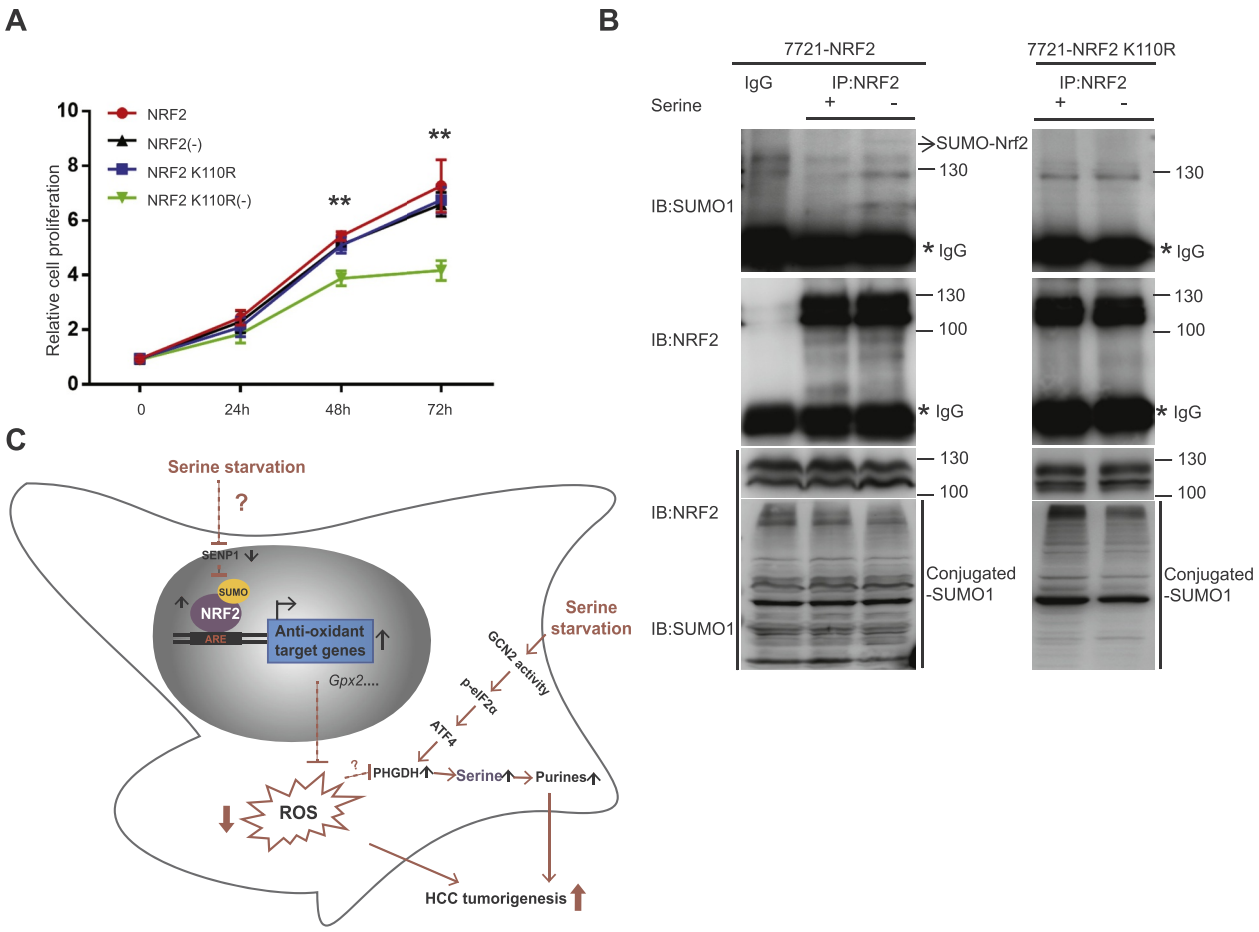

Fig. 6. NRF2 SUMOylation provides resistance to serine starvation in SMMC-7721 cells. **A**, Cells were cultured in DMEM supplemented with fetal bovine serum, but lacking serine and glycine for 72 h. Growth of the three cell types with and without serine was analyzed using the BrdU assay (3 replicates per group). **B**, Induction of Nrf2 SUMOylation in SMMC-7721-Nrf2 cells during serine starvation (immunoprecipitation assay). **C**, Summary model showing that Nrf2 K110 SUMOylation maintains HCC tumorigenesis by reducing the cellular level of ROS and increasing *de novo* serine synthesis to overcome serine starvation.

ATF4 pathway is critical for maintaining metabolic homeostasis and tumor progression during nutrient deprivation [43]. Ye et al. reported that this pathway up-regulates serine synthetic enzymes upon amino acid starvation of tumor cells [44]. In parallel to this pathway, we established that the NRF2 SUMOylation-GPX2-ROS axis in HCC cells regulated serine synthetic enzyme expression and SSP. Thus, under conditions of serine starvation, the GCN2-eIF2-ATF4 and NRF2 SUMOylation-GPX2-ROS pathways appear to contribute to the regulation of PHGDH at the transcriptional and translational levels.

In summary, we uncovered an apparently new pathway in which NRF2 SUMOylation promotes HCC tumorigenesis by enhancing *de novo* serine synthesis, and identified the SUMO1 conjugation site in NRF2 as lysine 110. By contributing to the removal of ROS and enhancing *de novo* serine synthesis, NRF2 K110 SUMOylation simultaneously helps HCC cells to tolerate oxidative stress and provides building blocks for tumorigenesis. Because tumor cells often experience fluctuating nutrient supplies, the role of NRF2 SUMOylation in regulating SSP to maintain HCC tumorigenesis seems more important during serine starvation. Maddocks et al. recently reported that dietary serine and glycine restriction had therapeutic effects in murine autochthonous tumors [45]. Thus, targeting NRF2 SUMOylation might be a potential therapy for HCC. Moreover, we also found that serine starvation reduced SENP1 expression in HCC cells (Fig. S8). This indicates the need to further examine the upstream signal pathways of cancer cells that regulate NRF2 SUMOylation in response to metabolic stress. We plan to use HCC murine models to further investigate the effect of serine restriction in combination with NRF2 K110 mutation as a novel therapeutic strategy for this cancer.

Author contributions

HYG, JQX, QZ, JLH, WZ, KZW carried out experiments and analyzed data. XH, QJF, JM and JKC provided administrative, technical, or material support. RC, RX and WHM designed the study, conceived the experiments and wrote the paper.

Acknowledgements

This work was supported by Natural Science Foundation of China (81572691, 81872230), National Basic Research Program of China (2015CB910400).

Appendix A. Supplementary data

Supplementary data to this article can be found online at https://doi.org/10.1016/j.canlet.2019.09.010.

Conflicts of interest

The authors declare no conflict of interest.

References

[1] M. Rojo de la Vega, E. Chapman, D.D. Zhang, NRF2 and the hallmarks of cancer,

Cancer Cell 34 (2018) 21–43.
[2] J.D. Hayes, A.T. Dinkova-Kostova, The Nrf2 regulatory network provides an interface between redox and intermediary metabolism, Trends Biochem. Sci. 39 (2014) 199–218.
[3] S.B. Lee, B.N. Sellers, G.M. DeNicola, The Regulation of NRF2 by Nutrient-responsive signaling and its role in anabolic cancer metabolism, Antioxid, Redox Signal 29 (2018) 1774–1791.
[4] Y. Mitsuishi, K. Taguchi, Y. Kawatani, T. Shibata, T. Nukiwa, H. Aburatani, M. Yamamoto, H. Motohashi, Nrf2 redirects glucose and glutamine into anabolic pathways in metabolic reprogramming, Cancer Cell 22 (2012) 66–79.
[5] A. Singh, C. Happel, S.K. Manna, G. Acquaah-Mensah, J. Carrerero, S. Kumar, P. Nasipuri, K.W. Krausz, N. Wakabayashi, R. Dewi, L.G. Boros, F.J. Gonzalez, E. Gabrielson, K.K. Wong, G. Girnun, S. Biswal, Transcription factor NRF2 regulates miR-1 and miR-206 to drive tumorigenesis, J. Clin. Investig. 123 (2013) 2921–2934.
[6] G.M. DeNicola, P.H. Chen, E. Mullarky, J.A. Sudderth, Z. Hu, D. Wu, H. Tang, Y. Xie, J. MAsara, K. EHuffman, I.I. Wistuba, J.D. Minna, R.J. DeBerardinis, L.C. Cantley, NRF2 regulates serine biosynthesis in non-small cell lung cancer, Nat. Genet. 47 (2015) 1475–1481.
[7] K. Schulze, S. Imbeaud, E. Letouze, L.B. Alexandrov, J. Calderaro, S. Rebouissou, G. Couchy, C. Meiller, J. Shinde, F. Soysouvanh, A.L. Calatayud, R. Pinyol, L. Pelletier, C. Balabaud, A. Laurent, J.F. Blanc, V. Mazzaferro, F. Calvo, A. Villanueva, J.C. Nault, P. Bioulac-Sage, M.R. Stratton, J.M. Llovet, J. Zucman-Rossi, Exome sequencing of hepatocellular carcinomas identifies new mutational signatures and potential therapeutic targets, Nat. Genet. 47 (2015) 505–511.
[8] Y. Totoki, K. Tatsuno, K.R. Covington, H. Ueda, C.J. Creighton, M. Kato, S. Tsuji, L.A. Donehower, B.L. Slagle, H. Nakamura, S. Yamamoto, E. Shinbrot, N. Hama, M. Lehmkuhl, F. Hosoda, Y. Arai, K. Walker, M. Dahdouli, K. Gotoh, G. Nagae, M.C. Gingras, D.M. Muzny, H. Ojima, Shimada, Y. Midorikawa, J.A. Goss, R. Cotton, A. Hayashi, J. Shibahara, S. Ishikawa, J. Guiteau, M. Tanaka, T. Urushidate, S. Ohashi, N. Okada, H. Doddapaneni, M. Wang, Y. Zhu, H. Dinh, T. Okusaka, N. Kokudo, T. Kosuge, T. Takayama, M. Fukayama, R.A. Gibbs, D.A. Wheeler, H. Aburatani, T. Shibata, Trans-ancestry mutational landscape of hepatocellular carcinoma genomes, Nat. Genet. 46 (2014) 1267–1273.
[9] Y. Inami, S. Waguri, A. Sakamoto, T. Kouno, K. Nakada, O. Hino, S. Watanabe, J. Ando, M. Iwadate, M. Yamamoto, M.S. Lee, K. Tanaka, M. Komatsu, Persistent activation of Nrf2 through p62 in hepatocellular carcinoma cells, J. Cell Biol. 193 (2011) 275–284.
[10] A. Petrelli, A. Perra, D. Cora, P. Sulas, S. Menegon, C. Manca, C. Migliore, M.A. Kowalik, G.M. Ledda-Columbano, S. Giordano, A. Columbano, MicroRNA/gene profiling unveils early molecular changes and nuclear factor erythroid related factor 2 (NRF2) activation in a rat model recapitulating human hepatocellular carcinoma (HCC), Hepatology 59 (2014) 228–241.
[11] P. Zavattari, A. Perra, S. Menegon, M.A. Kowalik, A. Petrelli, M.M. Angioni, A. Follenzi, L. Quagliata, G.M. Ledda-Columbano, L. Terracciano, S. Giordano, A. Columbano, Nrf2, but not beta-catenin, mutation represents an early event in rat hepatocarcinogenesis, Hepatology 62 (2015) 851–862.
[12] H.K.C. Ngo, D.H. Kim, Y.N. Cha, H.K. Na, Y.J. Surh, Nrf2 mutagenic activation drives hepatocarcinogenesis, Cancer Res. 77 (2017) 4797–4808.
[13] K.R. Mattaini, M.R. Sullivan, M.G. Vander Heiden, The importance of serine metabolism in cancer, J. Cell Biol. 214 (2016) 249–257.
[14] M. Yang, K.H. Vousden, Serine and one-carbon metabolism in cancer, Nat. Rev. Cancer 16 (2016) 650–662.
[15] G.M. DeNicola, F.A. Karreth, T.J. Humpton, A. Gopinathan, C. Wei, K. Frese, D. Mangal, K.H. Yu, C.J. Yeo, E.S. Calhoun, F. Scrimieri, J.M. Winter, R.H. Hruban, C. Iacobuzio-Donahue, S.E. Kern, I.A. Blair, D.A. Tuveson, Oncogene-induced Nrf2 transcription promotes ROS detoxification and tumorigenesis, Nature 475 (2011) 106–109.
[16] B. Chaneton, P. Hillmann, L. Zheng, A.C. LMartin, O.D.K. Maddocks, A. Chokkathukalam, J.E. Coyle, A. Jankevics, F.P. Holding, K.H. Vousden, C. Frezza, M2O'Reilly, E. Gottlieb, Serine is a natural ligand and allosteric activator of pyruvate kinase M2, Nature 491 (2012) 458–462.
[17] O.D. Maddocks, C.R. Berkers, S.M. Mason, L. Zheng, K. Blyth, E. Gottlieb, K.H. Vousden, Serine starvation induces stress and p53-dependent metabolic remodelling in cancer cells, Nature 493 (2013) 542–546.
[18] Y. Ou, S.J. Wang, L. Jiang, B. Zheng, W. Gu, p53 Protein-mediated regulation of phosphoglycerate dehydrogenase (PHGDH) is crucial for the apoptotic response upon serine starvation, J. Biol. Chem. 290 (2015) 457–466.
[19] M. Furukawa, Y. Xiong, BTB protein Keap1 targets antioxidant transcription factor Nrf2 for ubiquitination by the Cullin 3-Roc1 ligase, Mol. Cell. Biol. 25 (2005) 162–171.
[20] A. Kobayashi, M.I. Kang, H. Okawa, M. Ohtsuji, Y. Zenke, T. Chiba, K. Igarashi, M. Yamamoto, Oxidative stress sensor Keap1 functions as an adaptor for Cul3-based E3 ligase to regulate proteasomal degradation of Nrf2, Mol. Cell. Biol. 24 (2004) 7130–7139.
[21] D.V. Chartoumpekis, N. Wakabayashi, T.W. Kensler, Keap1/Nrf2 pathway in the frontiers of cancer and non-cancer cell metabolism, Biochem. Soc. Trans. 43 (2015) 639–644.
[22] S. Chowdhry, Y. Zhang, M. McMahon, C. Sutherland, A. Cuadrado, J.D. Hayes, Nrf2 is controlled by two distinct beta-TrCP recognition motifs in its Neh6 domain, one of which can be modulated by GSK-3 activity, Oncogene 32 (2013) 3765–3781.
[23] P. Rada, A.I. Rojo, S. Chowdhry, M. McMahon, J.D. Hayes, A. Cuadrado, SCF/{beta}-TrCP promotes glycogen synthase kinase 3-dependent degradation of the Nrf2 transcription factor in a Keap1-independent manner, Mol. Cell. Biol. 31 (2011) 1121–1133.
[24] H.C. Huang, T. Nguyen, C.B. Pickett, Phosphorylation of Nrf2 at Ser-40 by protein kinase C regulates antioxidant response element-mediated transcription, J. Biol. Chem. 277 (2002) 42769–42774.
[25] M.S. Joo, W.D. Kim, K.Y. Lee, J.H. Kim, J.H. Koo, S.G. Kim, AMPK facilitates nuclear accumulation of Nrf2 by phosphorylating at Serine 550, Mol. Cell. Biol. 36 (2016) 1931–1942.
[26] M.M. Talloy, D.J. McIntosh, T.S. Walters, A. Flores, J.S. Goodwin, I.J. Arinze, Trafficking of the transcription factor Nrf2 to promyelocytic leukemia-nuclear bodies: implications for degradation of NRF2 in the nucleus, J. Biol. Chem. 288 (2013) 14569–14583.
[27] K. Ramani, M.L. Tomasi, H. Yang, K. Ko, S.C. Lu, Mechanism and significance of changes in glutamate-cysteine ligase expression during hepatic fibrogenesis, J. Biol. Chem. 287 (2012) 36341–36355.
[28] K. Wang, W. Zhou, Q. Cai, J. Cheng, R. Cai, R. Xin, SUMOylation of KLF4 promotes IL-4 induced macrophage M2 polarization, Cell Cycle 16 (2017) 374–381.
[29] J.S. Seeler, A. Dejean, SUMO and the robustness of cancer, Nat. Rev. Cancer 17 (2017) 184–197.
[30] J. Cai, Y. Zuo, T. Wang, Y. Cao, R. Cai, F.L. Chen, J. Cheng, J. Mu, A crucial role of SUMOylation in modulating Sirt6 deacetylation of H3 at lysine 56 and its tumor suppressive activity, Oncogene 35 (2016) 4949–4956.
[31] I.I.C. Chio, S.M. Jafarnejad, M. Ponz-Sarvise, Y. Park, K. Rivera, W. Palm, J. Wilso, V. Sangar, Y. Hao, D. Öhlund, K. Wright, D. Filippini, E.J. Lee, B. Da Silva, C. Schoepfer, J.E. Wilkinson, J.M. Buscaglia, G.M. DeNicola, H. Tiriac, M. Hammell, H.C. Crawford, E.E. Schmidt, C.B. Thompson, D.J. Pappin, N. Sonenberg, D.A. Tuveson, NRF2 promotes tumor maintenance by modulating mRNA translation in pancreatic cancer, Cell 166 (2016) 963–976.
[32] M.L. Tomasi, M. Ryoo, H. Yang, A. Iglesias Ara, K. SKo, S. CLu, Molecular mechanisms of lipopolysaccharide-mediated inhibition of glutathione synthesis in mice, Free Radic. Biol. Med. 68 (2014) 148–158.
[33] S. Menegon, A. Columbano, S. Giordano, The dual roles of NRF2 in cancer, Trends Mol. Med. 22 (2016) 578–593.
[34] A. Arlt, S. Sebens, S. Krebs, C. Geismann, M. Grossmann, M.L. Kruse, S. Schreiber, H. Schäfer, Inhibition of the Nrf2 transcription factor by the alkaloid trigonelline renders pancreatic cancer cells more susceptible to apoptosis through decreased proteasomal gene expression and proteasome activity, Oncogene 32 (2013) 4825–4835.
[35] A.T. Dinkova-Kostova, A.Y. Abramov, The emerging role of Nrf2 in mitochondrial function, Free Radic. Biol. Med. 88 (2015) 179–188.
[36] R. Saddawi-Konefka, R. Seelige, E.T. Gross, E. Levy, S.C. Searles, A. Washington Jr., E.K. Santosa, B. Liu, T.E. O'Sullivan, O. Harismendy, J.D. Bui, Nrf2 induces IL-17D to mediate tumor and virus surveillance, Cell Rep. 16 (2016) 2348–2358.
[37] L. Bar-Peled, E.K. Kemper, R.M. Suciu, E.V. Vinogradova, K.M. Backus, B.D. Horning, T.A. Paul, T.A. Ichu, R.U. Svensson, J. Olucha, M.W. Chang, B.P. Kok, Z. Zhu, N.T. Ihle, M.M. Dix, P. Jiang, M.M. Hayward, E. Saez, R.J. Shaw, B.F. Cravatt, Chemical proteomics identifies druggable vulnerabilities in a genetically defined cancer, Cell 171 (2017) 696–709 e23.
[38] J.W. Locasale, A.R. Grassian, T. Melman, C.A. Lyssiotis, K.R. Mattaini, A.J. Bass, G. Heffron, C.M. Metallo, T. Muranen, H. Sharfi, A.T. Sasaki, D. Anastasiou, E. Mullarky, N.I. Vokes, M. Sasaki, R. Beroukhim, G. Stephanopoulos, A. HLigon, M. Meyerson, A.L. Richardson, L. Chin, G. Wagner, J.M. Asara, J.S. Brugge, L.C. Cantley, Phosphoglycerate dehydrogenase diverts glycolytic flux and contributes to oncogenesis, Nat. Genet. 43 (2011) 869–874.
[39] B. Zhang, A. Zheng, P. Hydbring, G. Ambroise, A.T. Ouchida, M. Goiny, H.3 Vakifahmetoglu-Norberg, E. Norberg, PHGDH defines a metabolic subtype in lung adenocarcinomas with poor prognosis, Cell Rep. 19 (2017) 2289–2303.
[40] S. Liu, Y. Sun, M. Jiang, Y. Li, Y. Tian, W. Xue, N. Ding, Y. Sun, C. Cheng, J. Li, X. Miao, X. Liu, L. Zheng, K. Huang, Glyceraldehyde-3-phosphate dehydrogenase promotes liver tumorigenesis by modulating phosphoglycerate dehydrogenase, Hepatology 66 (2017) 631–645.
[41] H.P. Harding, Y. Zhang, H. Zeng, I. Novoa, P.D. Lu, M. Calfon, N. Sadri, C. Yun, B. Popko, R. Paules, D.F. Stojdl, J.C. Bell, T. Hettmann, J.M. Leiden, D. Ron, An integrated stress response regulates amino acid metabolism and resistance to oxidative stress, Mol. Cell 11 (2003) 619–633.
[42] H.P. Harding, I. Novoa, Y. Zhang, H. Zeng, R. Wek, M. Schapira, D. Ron, Regulated translation initiation controls stress-induced gene expression in mammalian cells, Mol. Cell 6 (2000) 1099–1108.
[43] J. Ye, M. Kumanova, L.S. Hart, K. Sloane, H. Zhang, D.N. De Panis, D. Ron, C. Koumenis, The GCN2-ATF4 pathway is critical for tumour cell survival and proliferation in response to nutrient deprivation, EMBO J. 29 (2010) 2082–2096.
[44] J. Ye, A. Mancuso, X. Tong, P.S. Ward, J. Fan, J.D. Rabinowitz, C.B. Thompson, Pyruvate kinase M2 promotes de novo serine synthesis to sustain mTORC1 activity and cell proliferation, Proc. Natl. Acad. Sci. U. S. A. 109 (2012) 6904–6909.
[45] O.D.K. Maddocks, D. Athineos, E.C. Cheung, P. Lee, T. Zhang, N.J.F. van den Broek, Modulating the therapeutic response of tumours to dietary serine and glycine starvation, Nature 544 (2017) 372–376.